

More than just a Halogenase: Modification of Fatty Acyl Moieties by a Trifunctional Metal Enzyme

Sarah M. Pratter,^[a] Jakov Ivkovic,^[b] Ruth Birner-Gruenberger,^[c] Rolf Breinbauer,^[b] Klaus Zangger,^[d] and Grit D. Straganz^{*[a]}

The highly selective oxidative halogenations by non-heme iron and α -ketoglutarate-dependent enzymes are key reactions in the biosynthesis of lipopeptides, and often bestow valuable bioactivity to the metabolites. Here we present the first biochemical characterization of a putative fatty acyl halogenase, HctB, which is found in the hectochlorin biosynthetic pathway of *Lyngbya majuscula*. Its unprecedented three-domain structure, which includes an acyl carrier protein domain, allows self-contained conversion of the covalently tethered hexanoyl substrate. Structural analysis of the native product by ^{13}C NMR re-

veals high regioselectivity but considerable catalytic promiscuity. This challenges the classification of HctB as a primary halogenase: along with the proposed dichlorination, HctB performs oxygenation and an unprecedented introduction of a vinyl-chloride moiety into the nonactivated carbon chain. The relaxed substrate specificity is discussed with reference to a molecular model of the enzyme–substrate complex. The results suggest that fatty acyl transformation at the metal center of HctB can bring about considerable structural diversity in the biosynthesis of lipopeptides.

Introduction

Nonribosomal lipopeptides from bacterial, fungal or botanical sources with antimicrobial, anti-infective, and anticancer properties have been used for decades as potent pharmaceuticals. Because of their diversity, the exploration of these complex natural products is a popular and promising route for the discovery of new drugs. Many lipopeptides bear halogenated aliphatic moieties—modifications that strongly influence compound bioactivity.^[1] The molecular basis of this chemically challenging catalysis is a focus of this research.

Mononuclear non-heme iron (MNH) and α -ketoglutaric acid (α -KG)-dependent halogenases are arguably the most potent halogenating enzymes in nature, because of their unique ability to selectively transform carbon centers in nonactivated lipopeptide building blocks. MNH halogenases are generally found in polyketide synthase (PKS)/nonribosomal peptide synthetase (NRPS) pathways, and act on substrates that are tethered to

the thiolation domain of an acyl carrier protein (ACP) or peptidyl carrier protein (PCP) by a phosphopantetheinyl (PPT) moiety.^[1] Since the first report of an α -KG-dependent MNH halogenase,^[2] only a handful of representatives have been biochemically characterized.^[1,3–5] Analysis of the structure of *Pseudomonas syringae* threonyl halogenase SyrB2 has established the view that α -KG-dependent halogenases provoke halogenations because of a structural variation that sets them apart from the highly homologous ketoacid-dependent oxygenases: instead of the prototypical metal-binding facial triad of oxygenases (two histidines and one aspartate/glutamate), these halogenases have a small hydrophobic amino acid that substitutes for the carboxylic acid moiety and provides space for a chloride ion to coordinate to the iron.^[6] During the reaction mechanism, O_2 is activated and decarboxylates α -KG. The resulting high-valent $\text{Fe}^{\text{IV}}=\text{O}$ species abstracts a hydrogen atom, and a $\text{Cl}-\text{Fe}^{\text{III}}-\text{OH}$ species forms; in this, the chloride successfully competes with the hydroxy ligand for transfer to the substrate radical.^[1,7] This competition strongly depends on the positioning of the substrate relative to the $\text{Cl}-\text{Fe}^{\text{III}}-\text{OH}$ species.^[8]


Biochemical characterization of α -KG-dependent halogenases has mainly targeted monodomain enzymes that modify nonactivated amino acyl precursors. Another type of α -KG-dependent halogenase was found in a PKS/NRPS multi-domain protein and acts on activated carbon atoms: the JamE-halogenase domain (JamE-Hal) in the jamaicamide pathway chlorinates the γ -position of a 3-hydroxy-3-(4-pentynyl)glutaryl substrate, followed by a dehydratase and a decarboxylase, which transforms the α -hydroxyl halogen to a terminal vinyl-chloride moiety.^[3] The closely related cryptic halogenase CurA-Hal domain from the curacin A pathway, which is involved in the synthesis of a cyclopropyl moiety, shows similar enzymatic ac-

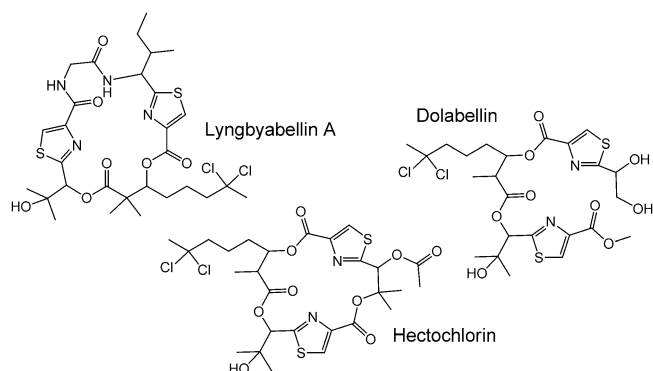
[a] S. M. Pratter, Dr. G. D. Straganz
Institute of Biotechnology and Biochemical Engineering
Graz University of Technology
Petersgasse 12, 8010 Graz (Austria)
E-mail: grit.straganz@tugraz.at

[b] J. Ivkovic, Prof. R. Breinbauer
Institute of Organic Chemistry, Graz University of Technology
Stremayrgasse 9, 8010 Graz (Austria)

[c] Prof. R. Birner-Gruenberger
Institute of Pathology and Center of Medical Research
Medical University of Graz
Stiftingtalstraße 24, 8010 Graz (Austria)

[d] Prof. K. Zangger
Institute of Chemistry, University of Graz
Heinrichstraße 28, 8010 Graz (Austria)

 Supporting information for this article is available on the WWW under <http://dx.doi.org/10.1002/cbic.201300345>.



Scheme 1. Examples of natural products with saturated halo fatty acyl moieties.

tivity.^[3] Yet, several bioactive natural products with long halogenated saturated alkyl chains are known (Scheme 1): hectochlorin and the related compounds dolabellin and lyngbyabellin A and B all harbor a 5,5-dichlorohexanoyl moiety;^[9] this suggests dihalogenation of a C₆ fatty acyl moiety. This implies a, so far uncharacterized, halogenase subtype, one that chlorinates nonactivated carbons in non-amino-acyl substrates. Genetic data of the hypothetical fatty acyl halogenase HctB from the hectochlorin pathway in *Lyngbya majuscula* indicate an unusual three-domain structure:^[9] an N-terminal catalytic halogenase domain, an acyl-coenzyme A binding protein (ACBP) domain of unknown function, and the substrate-anchoring ACP. The distinct three-module organization might be a common feature of fatty acyl halogenases, but so far only one other gene of similar organization has been reported,^[10] so more data will be needed to substantiate this.

Results and Discussion

The aim of this study was to explore the catalytic potential of the subfamily of MNH and α -KG-dependent fatty acyl halogenases that modify nonactivated medium-chain fatty acyl moieties. The catalytic metal center of an α -KG-dependent halogenase is in principle bifunctional, and the strong preference for chlorination over oxygenation is believed to be because of the substrate's precise positioning.^[8] Because unbranched, hydrophobic fatty acyl chains (presumably housed in "slippery" hydrophobic channels) are expected to show more flexibility than the small amino acid and 3-hydroxy-3-acyl-glutaryl building blocks of amino-acyl and keto-acyl halogenases, we were particularly interested in the chemo- and regioselectivities of fatty acyl halogenases. The first documented example of these for which the encoding gene cluster and natural product are known is HctB,^[9] the target enzyme of this work.

Production and spectral characterization of functional HctB

Because functional expression and reconstitution of multidomain proteins present special challenges, the purified enzyme was characterized in terms of its secondary structure, its competence to bind the cofactor, and the efficiency of substrate

loading. Full-length HctBs with an N- or C-terminal *Strep*-tag II were recombinantly expressed in *Escherichia coli*. Soluble protein was obtained only under an optimized procedure: fermentation at 18 °C and cell disruption with a buffer containing Na₂CO₃. SDS PAGE analysis confirmed the purity of HctB (> 95%) and the theoretical molecular weight (56.8 kDa; see Figure S1 in the Supporting Information). CD spectroscopy indicated properly folded protein with 24% α -helices, 25% β -sheets, 20% turns, and 30% unordered regions (Figure S2). Because of its higher protein yield (~40 mg L⁻¹ cell culture), the C-terminally tagged form was used for all following experiments. Spectrophotometric iron determination revealed 4–8% Fe^{II} in the isolated protein.

Enzymes from PKS/NRPS metabolic pathways typically require substrates that are covalently bound to a conserved serine residue, embedded in the thiolation domain of an ACP/PCP, by a PPT moiety. In the absence of an available native transferase, we chose the *Bacillus subtilis* enzyme Sfp,^[11] which is known to transfer a range of acyl-PPT moieties from respectively substituted coenzyme A (CoA) analogues, and covalently attach them to ACP domains from a variety of organisms. The PPT binding area of the ACP domain in HctB (Y-A-L-G-S-A-E) shows significant deviation from the consensus motif (L/V-G/L-G/A/F/Y-D/H/K/E-S-L/Q-D/A/G).^[12] Thus, in a first step, the principle ability of Sfp to transfer an acyl-PPT moiety onto HctB was assessed by a fluorescence-based method: incubation of ApoHctB with Sfp and BODIPY-CoA (which Sfp can competently transfer). Subsequent analysis by SDS PAGE demonstrated fluorescence labeling of HctB (Figure S3). Efficient modification of HctB with the PPT form of the native hexanoyl substrate was verified by MALDI-TOF MS analysis: the δ = 450 Da change in mass (from 56 785 to 57 235 Da) after the Sfp reaction is in line with the theoretical mass shift (438 Da) expected upon addition of the hexanoyl-PPT moiety to ApoHctB (56 778 Da), which gives hexanoyl-PPTylated HoloHctB (57 216 Da). No residual signal was found at m/z 56 785, thus demonstrating efficient transfer of the hexanoyl-PPT moiety to HctB (Figure S4).

Bidentate binding of the α -ketoacid cofactor to the Fe^{II} site is a prerequisite for O₂ activation in α -KG-dependent enzymes, and is characterized by the typical metal-to-ligand charge transfer (MLCT) band (approximately 530 nm).^[13] α -KG binding to the Fe^{II} core in HoloHctB was confirmed by anaerobic UV-vis spectrometry. Addition of 150 μ M α -KG to 300 μ M Fe^{II}-loaded HoloHctB resulted in a broad absorption band centered around 500 nm. With equimolar α -KG and Fe^{II}-HoloHctB, the extinction coefficient (ϵ_{490}) was approximately 125 M⁻¹ cm⁻¹; this did not increase upon addition of more α -KG. The band was present in both the absence (Figure S5) and presence of NaCl. This implies that the enzymatic Fe^{II} α -KG complex does not depend on the presence of chloride.

Characterization of HctB activity

Enzyme activity was determined by monitoring O₂ consumption in air-saturated enzyme preparations (260 μ M O₂) over time. In the absence of Fe^{II} or α -KG cofactors no oxygen depletion was detectable. In the presence of stoichiometric amounts

of Fe^{II} and $\alpha\text{-KG}$, HoloHctB displayed O_2 consumption rates that were essentially unchanged at higher $\alpha\text{-KG}$ concentrations (Figure S6B). Depending on the concentration of chloride, apparent first-order rate constants of O_2 depletion, $k_{\text{O}_2}^{\text{app}}$, ranged from $(0.42 \pm 0.21) \text{ min}^{-1}$ at less than 0.1 mM NaCl to $(12.11 \pm 4.11) \text{ min}^{-1}$ (average rate) at $\geq 1 \text{ M}$ NaCl (Figure 1A). The stoichiometry of O_2 consumption was characterized by determining the ratio of depleted O_2 to enzyme concentration (Fig-

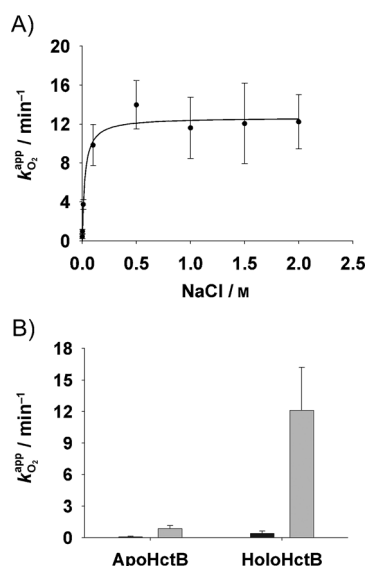


Figure 1. Dependency of HctB (100 μM) activity on substrate and chloride concentration in the presence of 150 μM Fe^{II} and 300 μM $\alpha\text{-KG}$ saturated conditions. A) Correlation of the apparent first order rate constants for HoloHctB ($k_{\text{O}_2}^{\text{app}}$) to NaCl concentration, and B) $k_{\text{O}_2}^{\text{app}}$ of ApoHctB and HoloHctB in the absence ($\leq 1 \text{ mM}$, black) or presence ($\geq 1 \text{ M}$, gray) of NaCl.

ure S7). $\alpha\text{-KG}$ addition and O_2 consumption were stoichiometric up to a concentration that corresponded to (1.91 ± 0.26) equivalents of HctB, and then reached a plateau. This is in line with a double oxidation of the ligand, whereby the employed HoloHctB is fully functional and O_2 consumption and substrate conversion are strongly coupled. When $\alpha\text{-KG}$ concentrations were more than one equivalent of enzyme, curves became biphasic with a slower phase ($k_{\text{O}_2}^{\text{app}} = 0.8 \pm 0.3 \text{ min}^{-1}$; Figure S6A), and the amplitudes of both phases became equal when $\alpha\text{-KG}$ concentration was two or more equivalents of enzyme. This might indicate distinct reaction rates for the first and second halogenation step. Full reaction rate and turnover was only achieved at more than 100 mM NaCl; at high chloride concentrations, as present in sea water,^[14] the enzymatic activity was maintained.

In halogenases, the presence of substrate has been found to be crucial for O_2 activation.^[7a,15] To test the necessity of substrate for HctB activity, the rates of O_2 consumption by ApoHctB were compared to those for HoloHctB (Figure S6A). In the absence of chloride, ApoHctB showed much reduced activity ($k_{\text{O}_2}^{\text{app}} = (0.08 \pm 0.06) \text{ min}^{-1}$). This basal rate increased approximately 11-fold in the presence of $\geq 1 \text{ M}$ chloride ($k_{\text{O}_2}^{\text{app}} =$

$(0.87 \pm 0.28) \text{ min}^{-1}$). In comparison, the presence of covalently linked substrate led to an approximately fivefold increase in O_2 consumption rate. Comparison of apo- and holoenzymes under NaCl saturation shows that covalently tethered substrate enhances enzymatic activity approximately 14 times. In contrast, addition of hexanoyl-CoA or hexanoic acid to ApoHctB did not significantly elevate O_2 consumption rates (in the absence or presence, respectively, of 1 M NaCl), thus indicating that covalent linkage of the substrate to HctB is required for activity. The strong impact of the chloride concentration on O_2 consumption rates (Figure 1) suggests that, in addition to substrate, chloride is required for efficient primary O_2 activation in HctB. This is the first time that the impact of chloride concentration on O_2 consumption rates of a non-heme iron halogenase has been reported; current investigations aim at clarifying the role of chloride regarding O_2 reduction in HctB.

The catalytic and ACP domains in HctB are separated by an ACBP of unknown function. For homologous ACBPs, a role as an intracellular acyl-CoA transporter has been ascribed; involvement in intermediary metabolism and gene regulation in various organisms has also been proposed.^[16] In order to test for a regulatory role of this high-affinity acyl-CoA binding domain during catalysis, HoloHctB activity in the presence of a variety of acyl-CoAs was investigated. However, addition of stoichiometric hexanoyl-CoA, octanoyl-CoA, decanoyl-CoA, lauryl-CoA, or myristoyl-CoA did not significantly impact the O_2 consumption characteristics of the enzyme. (Note that MALDI-TOF MS data showed no presence of a tightly bound acyl-CoA ligand in HoloHctB preparations; this might have masked an impact of acyl-CoAs on activity in our assay).

Catalytic promiscuity

MALDI-TOF MS analysis of HoloHctB revealed shifts in m/z of approximately 70 and 160 after conversions with chloride and bromide, respectively, when compared to an unconverted HoloHctB control sample (Figure S8). The observed mass shifts were consistent with dihalogenation of the substrate. Because of the low resolution of the method, however, the presence of a mixture of products with distinct masses could not be ruled out.

To qualitatively identify the native reaction products, the HoloHctB acyl-moieties were hydrolyzed from their enzyme-bound PPT arm after conversion by the thioesterase TycF,^[17] and tested for modifications by using a coupled HPLC-MS technique. Product solutions of NaCl-containing reactions, NaCl-free reactions, and unconverted Fe^{II} - and $\alpha\text{-KG}$ -free controls were scanned for particular m/z values. Samples from NaCl-saturated HoloHctB conversions showed species of m/z 129, 147, and 183 (corresponding to oxohexanoate, monochlorohexanoate, and dichlorohexanoate, respectively). No significant amounts of hexanoate (the only species present in unconverted HoloHctB samples) were found. In an "NaCl-free" conversion (chloride was avoided for sample and buffer preparations), hexanoate and oxohexanoate were detected. Furthermore, traces of monochlorohexanoate, monochlorohexenoate, and dichlorohexanoate were found, probably because of un-

avoidable contamination of buffers with trace chloride. Additionally a captured ion at 8.8 min in both NaCl-free and NaCl-saturated samples was consistent with a monohydroxyhexanoate species (m/z 131), but could not be unambiguously identified because of a lack of available standards (signals of the detected ions are in Figure S9). The presence of chloride in the reaction products was verified by its prototypical isotope pattern. The statistically expected molecular weight ratio for monochlorinated substances ($^{35}\text{Cl}/^{37}\text{Cl}$, 3.1:1) and for dichlorinated substances ($^{35}\text{Cl}_2/^{35}\text{Cl}^{37}\text{Cl}/^{37}\text{Cl}_2$, 9.8:6.3:1) was found for the elution peaks at $t=33.8$ and 37.7 min; this confirmed their tentative identifications as monochlorohexenoate and dichlorohexanoate, respectively (Figure S10).

To gain more structural information on the reaction products, acyl moieties with a fully ^{13}C -labeled hexanoyl backbone were employed. [$^{13}\text{C}_6$]hexanoyl-CoA was obtained by oxidation of [$^{13}\text{C}_6$]hexan-1-ol and subsequent enhanced S-acylation to CoA by an established method^[18] (Scheme S1) with a total yield of 36%. [$^{13}\text{C}_6$]-labeled products were subjected to NMR analysis in two ways: 1) still bound to HctB and, 2) hydrolyzed and separated from the enzyme. ^1H , ^{13}C HSQC of the unconverted ^{13}C -labeled hexanoyl moiety attached to HctB showed the expected broad NMR signals because of the large molecular weight. After the enzymatic reaction, a number of additional peaks were found; these were assigned after cleavage from the enzyme by recording one-dimensional ^{13}C and two-dimensional ^1H , ^{13}C HSQC and INADEQUATE spectra (Figure S11). The assignment was corroborated by comparison with ^{13}C and ^1H , ^{13}C HSQC spectra of hexanoic acid, 5-oxo-hexanoic acid, 6-chloro-hexanoic acid, and published values for 5,5-dichlorohexanal.^[19] For semiquantitative analysis of the relative amounts of the individual free products, ^{13}C spectra with long relaxation delays (5 s) were recorded; intensity comparisons were performed only for signals of the same multiplicity. From these, the amount of hexanoyl substrate was determined to be approximately 10%, thus indicating almost quantitative conversion. Identified reaction products confirmed the results from the HPLC-MS analysis: 5-oxo-hexanoic acid (~50%), 5,5-dichlorohexanoic acid (~25%), and 5-chlorohex-4-enoic acid (~25%). No signals for monohydroxyhexanoate were found, thus indicating that this is only a minor product component (representative ^{13}C spectrum of free products in Figure 2A). Products identified in the free form were also found bound to the protein, where they show markedly increased line widths because of the significantly increased molecular weight of the enzyme. (An overlay of an HSQC of free products and products bound to HctB is shown in Figure 2B.) Product spectra did not significantly change for samples that were stored for several weeks at room temperature, thus indicating chemical stability of the compounds under these conditions.

The impact of chloride concentration on the product spectrum was assessed by HPLC-MS analysis. The relative concentrations of 5,5-dichloro-hexanoic acid and 5-chloro-4-hexenoic acid were unchanged over the whole investigated range (0–1 M NaCl). The proportion of 5-oxo-hexanoic acid remained constant down to 35 mM NaCl. It was, however, significantly elevated in the salt-free sample, along with species whose

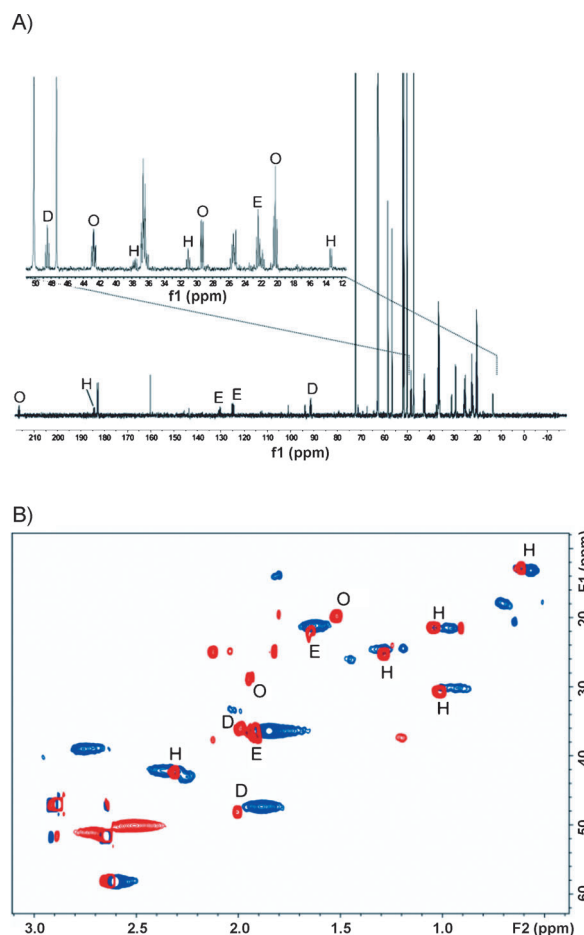


Figure 2. ^{13}C NMR spectra of HctB reaction products. A) One-dimensional ^{13}C NMR spectrum of free hexanoyl products. Non-overlapped signals of the individual products are labeled: H (hexanoic acid), O (5-oxohexanoic acid), E (5-chlorohex-4-enoic acid), and D (5,5-dichlorohexanoic acid). The observed carbon–carbon couplings arise from the use of uniformly ^{13}C -labeled hexanoic acid precursors and make the product peaks easily distinguishable from the strong singlets of the buffer (HEPES). A spectrum with longer relaxation time is given in Figure S15. B) Overlay of ^1H , ^{13}C HSQC spectra of free products (red) and products bound to HctB (blue).

masses and isotope distributions were consistent with monohydroxylated and monochlorinated products (Figure S12).

In summary, product analysis revealed remarkable catalytic promiscuity. Intriguingly, beside dihalogenation and oxygenation, an unprecedented introduction of vinyl chloride into the nonactivated fatty acyl chain was observed, whereby regioselectivity was retained. This incorporation of a nonterminal vinyl chloride moiety into a nonactivated carbon chain by a single enzyme contrasts with the previously described MNH-dependent methylene-chloride formation in jamaicamides,^[3] where conversion is accomplished by three enzymes and is restricted to activated substrates and the synthesis of terminal vinyl chlorides.

Substrate and halogen promiscuity

HctB displayed a remarkable promiscuity with alternative fatty acyl substrates. HoloHctB variants that carried an octanoyl-,

decanoyl-, lauryl-, or myristoyl group instead of the native hexanoyl substrate showed considerable O_2 consumption rates. However, the rates decreased with growing chain length: an approximately fivefold drop for the myristoyl moiety ($k_{O_2}^{app} = 2.4 \pm 1.0 \text{ min}^{-1}$), compared to the native substrate (Figure 3A)

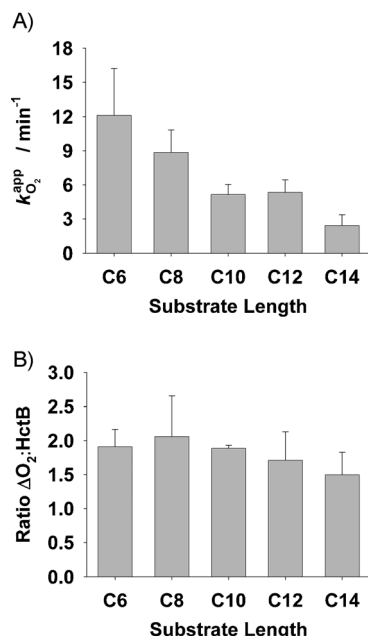


Figure 3. HctB activity towards putative alternative fatty acyl substrates. A) Apparent first order rate constants and B) O_2 consumption stoichiometry of hexanoyl (C₆)-, octanoyl (C₈)-, decanoyl (C₁₀)-, lauryl (C₁₂)-, and myristoyl (C₁₄)-HoloHctB under cofactor saturating conditions.

was observed. O_2 consumption stoichiometry did not change significantly (Figure 3B). The principle potential of HctB for bromination in the presence of 1 M KBr was confirmed as analogous to amino acyl halogenases;^[20] rates were approximately four times slower ($k_{O_2}^{app} = (3.0 \pm 1.1) \text{ min}^{-1}$) than for the respective chlorination reaction, and O_2 consumption stoichiometry suggested less than two conversions (Figure S13).

In order to rationalize the surprisingly relaxed substrate spectrum, a structural model of the HctB catalytic domain was generated and subjected to in silico docking of acyl-PPT moieties. Similar, low-energy positioning was found in the vicinity of the catalytic metal center for all docked fatty acyl moieties (Figure 4). The C4–C6 carbon atoms of the native substrate were close to the chloride ion (3.5–4.5 Å) and to the iron (~6–7 Å), and, in general, all ligands exposed their carbon chains to the active center (3.4–6.3 Å to the chloride, 5.3–8.1 Å to the metal). This is in good agreement with experimental data, which suggests that C₈–C₁₄ acyl chains induce primary O_2 activation. In halogenases substrate binding has been found to replace a water ligand from the iron, presumably in the vicinity of the substrate and metal ion. This leads to a five-coordinate iron center that is competent to reduce O_2 . Docking of the ACP domain to the catalytic domain results in a low energy form, where the conserved Ser427 of the thiolation domain is

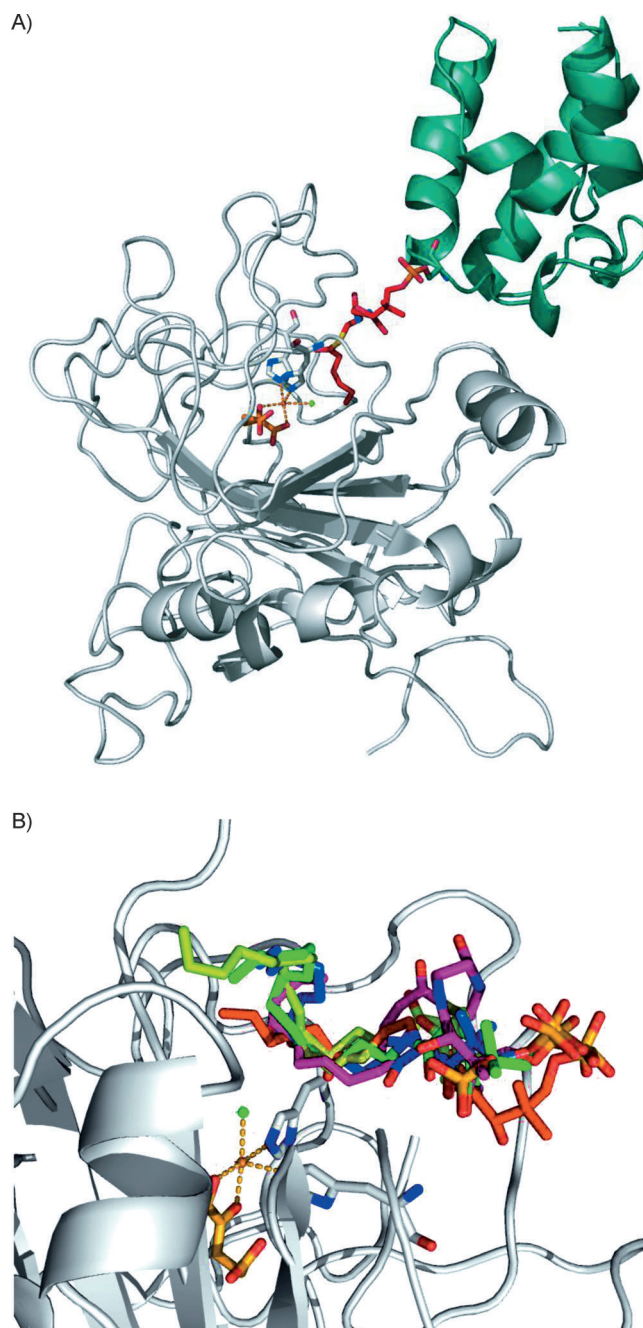


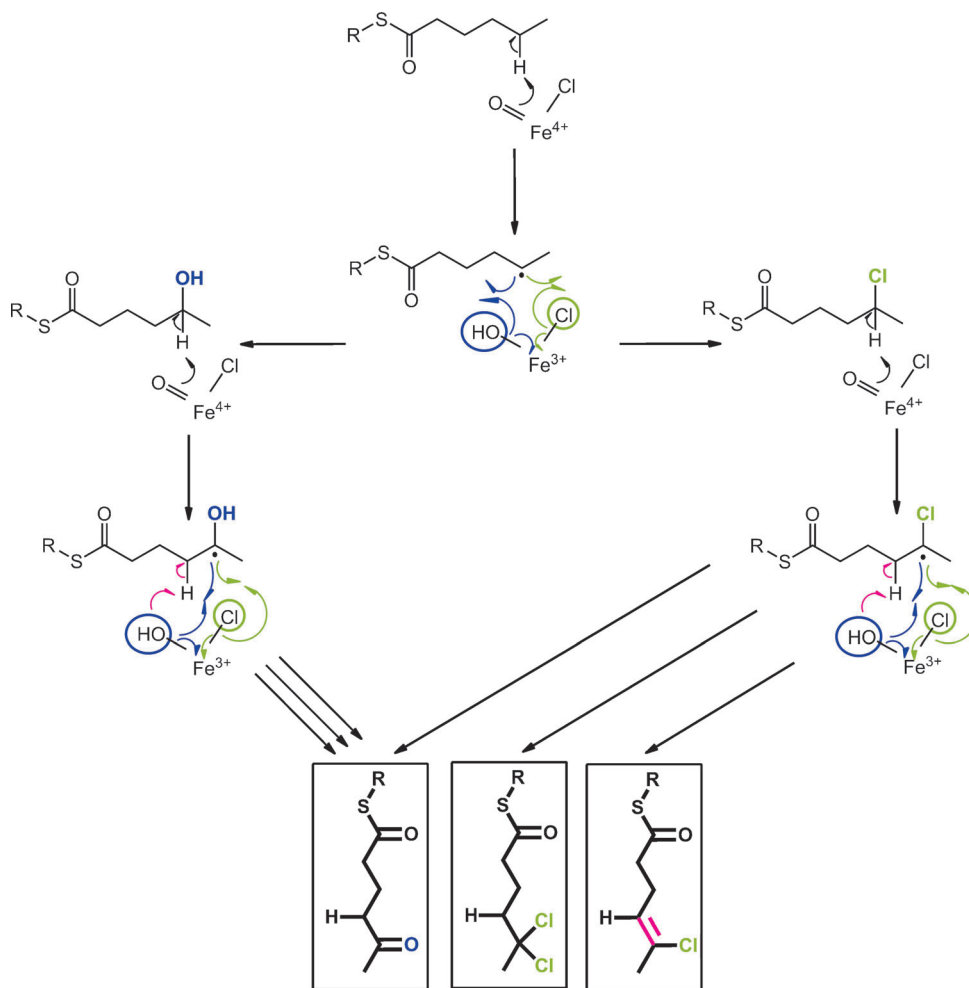
Figure 4. Structural model of the HctB Hal-ACP-substrate complexes. A) Overall structural model of a catalytic domain and ACP domain (green) with the native C₆ substrate after covalent linkage of the hexanoyl-PPT and ACP domain and its relaxation by MD simulation. B) Close-up of the docking results for C₆–C₁₄ substrates (residues 1–14 and 223–226 omitted for clarity). C₆ (red), C₈ (blue), C₁₀ (green), C₁₂ (yellow), and C₁₄ (violet). PPT-acyl-substrates were docked into a model of the HctB catalytic domain (gray) containing the metal coordinating histidines (gray sticks), the iron cofactor (orange ball), a chloride atom (green ball), and the α-KG cofactor (orange sticks).

less than 6 Å from the terminal PPT-phosphate moiety. The resulting two-domain model contradicts a previously proposed role of the ACBP domain in substrate binding during catalysis.^[10]

Conclusions

Multifunctionality, including desaturase activity, has already been reported for α -KG-dependent MNH enzymes (e.g., clavaminic synthase).^[21] α -KG-dependent halogenases have been shown to halogenate their native substrates: nonquantitated amounts of hydroxylation were reported in SyrB2 and these were elevated in non-native substrate analogues.^[8] The introduction of a vinyl-chloride moiety into a nonactivated carbon chain, as reported herein, is to the best of our knowledge, unprecedented. The structure of hectochlorine,^[9] together with the classification of the preceding acyl-ACP-synthetase HctA according to sequence alignment,^[22] strongly suggests that the hexanoyl moiety is indeed the natural substrate of HctB, and that chain length specificity is determined by HctA. Our study suggests that a multifunctional metal center in HctB might introduce structural variety into the primary building block of hectochlorin by dichlorination, oxygenation, and vinyl-chloride formation. The product pattern of HctB under chloride-saturating conditions displays chloride and oxo moieties exclusively at the C5 position, a double bond C4=C5. Furthermore, strong coupling of α -KG consumption to O₂ depletion is observed, which, however, does not exceed two turnovers. Based on these findings and previously suggested mechanisms for α -KG-dependent halogenases and oxygenases, we propose a reaction mechanism where initial transfer of either a metal-bound hydroxyl or chloride species at C5 takes place; in a second oxidation cycle, the remaining hydrogen at C5 is abstracted. The comparatively stable radical might then undergo a second chlorination/hydroxylation reaction or, alternatively, the intermediate Cl-Fe^{III}-OH moiety might abstract a hydrogen atom from C4 to give the three observed reaction products (Scheme 2).

In summary, the catalytic properties of HctB imply that the product spectrum obtained by the hectochlorin pathway in *L. majuscula* comprises structural variants with oxo- and vinyl-chloride alkyl chains and, by extension, that examples of the acyl-halogenase group generally display all three functionalities in equal measure. This is in line with the observation that biological lipopeptide pathways often employ promiscuous en-



Scheme 2. Proposed mechanism of product formation by HctB. In the first oxidation cycle, the hexanoyl substrate is chlorinated or hydroxylated at C5. In the second round, a radical at C5 is again generated; this binds either the chloride or the hydroxyl moiety to yield dichloro- or oxo-hexanoate, or abstracts a proton from the vinyl-chloride product.

zymes that generate a range of reactions products, which are then assembled into a variety of metabolites. The resulting structural diversity of the secondary metabolites increases the chances of producing a bioactive variant that bestows evolutionary fitness.^[23]

Experimental Section

Chemicals: If not otherwise stated, chemicals were purchased from Sigma-Aldrich or Carl Roth at the highest purity available. Phusion DNA Polymerase, pKYB1 vector, and T4 DNA ligase were from New England BioLabs (Ipswich, MA) and restriction enzymes and buffers, and alkaline phosphatase from Fermentas (Thermo Scientific).

Cloning: The *hctB* gene was synthesized based on the hectochlorin biosynthetic gene cluster (accession number AY974560). Therefore the sequence that codes for HctB (AY974560 is the DNA accession number to the complete sequence of the hectochlorin biosynthetic gene cluster in *Lyngbya majuscula*, no accession number for *hctB* only is available), was C-terminally appended with a *Strep*-tag II

(WSHPQFEK), flanked with NdeI and BamHI restriction sites, and codon optimized for expression in *E. coli*; the PPT-transferase *sfp* sequence from *B. subtilis*^[11] (accession AEK64474.1) was C-terminally His₆-tagged; both constructs were purchased from Mr. Gene GmbH, Regensburg, Germany). C-terminally tagged *hctB* was cut from the purchased plasmid and cloned into vector pKYB1 (New England Biolabs) by using the vector's NdeI and BamHI restriction sites. His-tagged *sfp* was flanked with NdeI and BamHI restriction sites by PCR, digested with the respective enzymes, and also cloned into a pKYB1 vector. The N-terminally *Strep*-tag II-tagged *hctB* construct was prepared by flanking the *hctB* sequence with BsaI by using the PCR technique, a subsequent restriction digest and cloning into the respective site of the pASK-IBA7plus vector (IBA, Göttingen, Germany) according to the manufacturer's procedures. Construct integrity was confirmed by sequencing (Eurofins MWG Operon, Ebersberg, Germany).

Protein expression: The above plasmids and pET30a_TycF (the plasmid bearing the N-terminally His₆-tagged tycF thioesterase gene) were introduced into *E. coli* BL21 Gold (DE3) cells by electroporation. HctB expression was performed in a medium that had previously been optimized for the expression of a MNH dioxygenase.^[24] Expression cultures (300 mL) were inoculated with overnight culture (to OD₆₀₀ = 0.1–0.2) and allowed to grow (37 °C, 110 rpm). At OD₆₀₀ ≈ 0.7, protein expression was induced by addition of IPTG (100 µg mL⁻¹). After incubation (18 °C, 22 h), cells were harvested and resuspended in AP2 buffer (Tris (50 mM, pH 8.5), NaCl (150 mM), Na₂CO₃ (100 mM), glycerol (5%)). Sfp and TycF were both produced in 2 × YT. Sfp was expressed according to the HctB protocol but at 25 °C and with resuspension in TMGD buffer (pH 6.9)^[11] TycF was expressed as previously described.^[17]

Protein purification: Cells were disrupted by two passages through a French press (~24 000 psi). After removal of cell debris (78 000 g, 35 min, 4 °C), soluble *Strep*-tagged HctB was purified on a *Strep*-Tactin Superflow column (IBA) according to the manufacturer's instructions, and buffer exchanged into HEPES (20 mM, pH 7.5). His-tagged Sfp and TycF were purified by affinity chromatography on a self-packed Cu-chelat column (Chelating Sepharose Fast Flow, GE Healthcare) with a stepwise imidazole gradient (Tris (50 mM, pH 7.5), NaCl (300 mM), imidazole (0–400 mM)). TycF was buffer exchanged into HEPES (20 mM, pH 7.5); Sfp was buffer exchanged into TMGD (pH 6.9). Cell disruption, affinity chromatography, buffer exchange, and concentration of protein samples (Vivaspin 20; Sartorius, Tagelsungen, Switzerland) were performed at 4 °C. The protein concentration of HctB was determined by a modified procedure of Edelhoch and Pace.^[25] Concentrations of Sfp and TycF were determined by using the Bio-Rad Protein Assay (Bio-Rad, Hercules, CA). The purity of the isolated enzymes and their molecular weights were verified by SDS-PAGE (GE Healthcare; see Figures S1 and S14).

Fe^{II} content: The quantity of Fe^{II} in HctB preparations was determined photometrically at 25 °C in Tris-HCl (20 mM, pH 7.5) according to the method of Hennessy et al.^[26] by using ~350-fold molar excess of Ferene-S (3-(2-pyridyl)-5,6-di(2-furyl)-1,2,4-triazine-5',5''-disulfonic acid) Detachment of iron from the native protein and concomitant formation of the colored Fe^{II}-Ferene-S complex (ϵ_{592} = 35.5 mm⁻¹ cm⁻¹) was monitored over 15–18 h.

Circular dichroism (CD) spectroscopy: Far-UV CD spectra were recorded on a J-715 spectropolarimeter (Jasco; RT, 0.02 cm path length, cylindrical cell) as described previously,^[27] with enzymes (~0.40 mg mL⁻¹) in potassium phosphate (20 mM, pH 7.5). Three spectra (300–185 nm) were averaged and corrected by a blank

spectrum (lacking enzyme) before converting the CD signal into mean residue ellipticity. Data were processed at the DichroWeb server (<http://dichroweb.cryst.bbk.ac.uk>).^[28]

Reconstitution of HoloHctB: Aliquots of ApoHctB (200–500 nmol) were mixed with Sfp (0.1 equiv) and the respective fatty acyl CoA (C₆–C₁₄, 2 equiv) in transfer buffer (Tris-Cl (75 mM, pH 7.5), MgCl₂ (10 mM)), to a final HctB concentration of 200–500 µM. Reaction mixtures were incubated on a thermo-shaker (24 °C, 350 rpm, 1–1.5 h). Precipitated protein was removed by centrifugation prior to buffer exchange to either Tris-H₂SO₄ (20 mM, pH 7.5) or HEPES/NaOH, (20 mM, pH 7.5). HoloHctB samples were concentrated (~two- to fivefold), and protein concentrations were reassessed.

Bodipy-CoA transfer assay: Bodipy-CoA was prepared according to La Clair et al.^[29] and then transferred (as described for fatty acyl substrates). Samples were subjected to SDS PAGE and analyzed by a fluorescence scanner (Bio-Rad; λ_{ex} = 532 nm, λ_{em} = 555 nm) with a long pass filter.

Mass spectrometry: Purified protein solutions were desalted by repeated cycles of concentration and dilution in TFA (0.1%) by using 10 kDa cut off Amicon ultrafiltration tubes (Merck Millipore), then diluted (1:10, v/v) in acetonitrile (50%) and TFA (0.1%), and mixed (1:1, v/v) with super-DHB matrix (5 mg; 9:1 mixture of 2,5-dihydroxybenzoic acid and 2-hydroxy-5-methoxybenzoic acid) in acetonitrile (50 µL) and TFA (50 µL, 0.1%). Samples (1 µL) were spotted onto an 800 µm MTP AnchorChip (Bruker) and left to dry. MALDI-TOF-MS measurements were performed on an ultrafleXtreme spectrometer (Bruker). Full MS spectra were obtained in positive linear mode (mass/charge range 8000–77 000) after external calibration with the appropriate protein standard (10–70 kDa).

α -KG binding: Anaerobic HoloHctB samples (300 µM) in the absence or presence of NaCl (1 M) were prepared in HEPES/NaOH (20 mM, pH 7.5) in air-tight NextGen V Vials with septa-sealed open-top screw caps (Wheaton Millville, NJ, USA), and purged with nitrogen. Residual O₂ was consumed by adding an equimolar amount of acetylacetone, and depleting with the dioxygenase Dke1 (4–5 µM), which is available in our lab.^[27] Nitrogen-flushed, O₂-free Fe^{II} and α -KG cofactors were added as stock solutions in microliter quantities in an N₂-purged glove box to yield 300 µM Fe^{II} and 0, 150, 300, or 600 µM α -KG. Spectra (250–800 nm) were recorded on a CARY 50 Bio UV/Vis Spectrophotometer (Varian/Agilent Technologies). Three replicates (1200 nm min⁻¹) were performed for each condition and averaged for analysis.

HctB activity assay: Apo- and HoloHctB activities were recorded by monitoring O₂ consumption over time with a luminescence-based Needle-Type Oxygen Microsensor (Type Pst1) (PreSens, Regensburg, Germany) in an air-tight cell. Enzymes (100 µM) were tested with stirring at 23 °C in either Tris-H₂SO₄ (500 µL, 20 mM, pH 7.5) or HEPES/NaOH (500 µL, 20 mM, air-saturated, pH 7.5) supplemented with NaCl (0–2 M) or KBr (1 M). α -KG was added as an air-saturated aqueous stock solution (5–100 mM, final concentration 50–1000 µM); Fe^{II} was added as an anaerobic aqueous stock solution (15 mM, final concentration 150 µM). Reaction rates of substrate turnover at 260 µM O₂ ($k_{\text{O}_2}^{\text{app}}$) were calculated based on fits to a single ($f = y_0 + ae^{(-bx)}$) or double ($f = y_0 + ae^{(-bx)} + ce^{(-dx)}$) exponential decay (Sigma Plot 9.0), where y_0 is the final O₂ concentration after conversion, a and c are the amplitudes of the curve, b and d are the respective $k_{\text{O}_2}^{\text{app}}$ and $k_{\text{O}_2}^{\text{app}}$ values, and x is time in seconds. Determined rates were validated by using the initial reaction rate divided by the protein concentration.

Isolation of reaction products: HoloHctB samples from activity assays were pooled, buffer exchanged into HEPES/NaOH (20 mM, pH 7.5), and concentrated to ~1 mM. Acyl-moiety cleavage from the enzyme ACP domain was accomplished by incubating (30 °C, 350 rpm, overnight) with thioesterase TycF^[17] (15–30 μM). Precipitated protein was removed by centrifugation. The supernatant was subjected to a VivaSpin 500 centrifugal filter (Sartorius) and the filtrate, which contained the cleaved carbonic acid, was collected. Samples for ¹³C NMR analysis were supplemented with deuterium oxide (10%).

HPLC-MS analysis: Reaction products (cleaved from the enzyme) and standard solutions of hexanoic acid, 5-oxo-hexanoic acid, and 6-chloro hexanoic acid were acidified with formic acid (FA; 1%, v/v). HPLC analysis was performed with a 1200 Infinity Series system (Agilent Technologies) and a LiChroCART Purospher STAR column (Merck Millipore; 30 °C, 0.8 mL min⁻¹) with FA (1% in water; solvent A) and FA (1% in acetonitrile; solvent B): 10% B (10 min), 10–50% B (30 min), 50–90% B (1 min), 90% B (3 min), 90–10% (1 min), 10% B (10 min). Separated components were analyzed by ESI-MS single ion monitoring (SIM) in a negative ion detection mode.

Synthesis of [¹³C₆]-labeled acyl-CoA: The synthesis of [¹³C₆]hexanoyl-CoA was from commercially available [¹³C₆]hexan-1-ol (Sigma-Aldrich). A microscale model synthesis was developed first with unlabeled hexan-1-ol. [¹³C₆]Hexanoyl-CoA was obtained in a total yield of 36% by oxidation of [¹³C₆]hexan-1-ol^[30] and subsequent enhanced S-acylation to CoA by a published method^[18] with PyBOP as the coupling agent (Scheme S1).

NMR analysis: ¹³C-labeled enzyme–product complexes and hydrolyzed reaction products were analyzed on an Avance III 700 MHz NMR spectrometer (298 K; Bruker) equipped with a 5 mm TCI cryo probe. For the one-dimensional ¹³C NMR spectra, 16384 scans were acquired in 8.5 h; ¹H,¹³C HSQCs were recorded with 16 scans for each of the 128 increments. For INADEQUATE spectra, 512 scans were accumulated for each of the 64 transients.

HctB structural modeling and in silico docking: A structural model of the HoloHctB halogenase and ACP domains was generated by a combination of in silico docking and MD simulations (see the Supporting Information).

Acknowledgements

The *tycF*-containing *pET30a* plasmid was a kind gift from the group of Chris T. Walsh, Harvard Medical School (USA). Financial support by the Austrian Science Fund (FWF) grant W901-B05 DK Molecular Enzymology is gratefully acknowledged.

Keywords: halogenation • metalloenzymes • molecular diversity • natural products • non-heme iron

- [3] L. Gu, B. Wang, A. Kulkarni, T. W. Geders, R. V. Grindberg, L. Gerwick, K. Håkansson, P. Wipf, J. L. Smith, W. H. Gerwick, D. H. Sherman, *Nature* **2009**, 459, 731–735.
- [4] W. Jiang, J. R. Heemstra Jr., R. R. Forseth, C. S. Neumann, S. Manaviazar, F. C. Schroeder, K. J. Hale, C. T. Walsh, *Biochemistry* **2011**, 50, 6063–6072.
- [5] C. S. Neumann, C. T. Walsh, *J. Am. Chem. Soc.* **2008**, 130, 14022–14023.
- [6] L. C. Blasiak, F. H. Vaillancourt, C. T. Walsh, C. L. Drennan, *Nature* **2006**, 440, 368–371.
- [7] a) M. L. Matthews, C. M. Krest, E. W. Barr, F. H. Vaillancourt, C. T. Walsh, M. T. Green, C. Krebs, J. M. Bollinger Jr., *Biochemistry* **2009**, 48, 4331–4343; b) C. Krebs, D. Galonić Fujimori, C. T. Walsh, J. M. Bollinger Jr., *Acc. Chem. Res.* **2007**, 40, 484–492; c) D. P. Galonić, E. W. Barr, C. T. Walsh, J. M. Bollinger Jr., C. Krebs, *Nat. Chem. Biol.* **2007**, 3, 113–116.
- [8] M. L. Matthews, C. S. Neumann, L. A. Miles, T. L. Grove, S. J. Booker, C. Krebs, C. T. Walsh, J. M. Bollinger Jr., *Proc. Natl. Acad. Sci. USA* **2009**, 106, 17723–17728.
- [9] A. V. Ramaswamy, C. M. Sorrels, W. H. Gerwick, *J. Nat. Prod.* **2007**, 70, 1977–1986.
- [10] A. Nishizawa, A. B. Arshad, T. Nishizawa, M. Asayama, K. Fujii, T. Nakano, K.-i. Harada, M. Shirai, *J. Gen. Appl. Microbiol.* **2007**, 53, 17–27.
- [11] L. E. N. Quadri, P. H. Weinreb, M. Lei, M. M. Nakano, P. Zuber, C. T. Walsh, *Biochemistry* **1998**, 37, 1585–1595.
- [12] R. H. Lambalot, A. M. Gehring, R. S. Flugel, P. Zuber, M. LaCelle, M. A. Marahiel, R. Reid, C. Kohsla, C. T. Walsh, *Chem. Biol.* **1996**, 3, 923–936.
- [13] M. J. Ryle, R. Padmakumar, R. P. Hausinger, *Biochemistry* **1999**, 38, 15278–15286.
- [14] M. Lefort-Tran, M. Pouphe, S. Spath, L. Packer, *Plant Physiol.* **1988**, 87, 767–775.
- [15] M. L. Neidig, C. D. Brown, K. M. Light, D. G. Fujimori, E. M. Nolan, J. C. Price, E. W. Barr, J. M. Bollinger Jr., C. Krebs, C. T. Walsh, E. I. Solomon, *J. Am. Chem. Soc.* **2007**, 129, 14224–14231.
- [16] J. Knudsen, S. Mandrup, J. T. Rasmussen, P. H. Andreasen, F. Poulsen, K. Kristiansen, *Mol. Cell. Biochem.* **1993**, 123, 129–138.
- [17] E. Yeh, R. M. Kohli, S. D. Bruner, C. T. Walsh, *ChemBioChem* **2004**, 5, 1290–1293.
- [18] W. Zhang, M. L. Bolla, D. Kahne, C. T. Walsh, *J. Am. Chem. Soc.* **2010**, 132, 6402–6411.
- [19] H. Sone, T. Kondo, M. Kiryu, H. Ishiwata, M. Ojika, K. J. Yamada, *J. Org. Chem.* **1995**, 60, 4774–4781.
- [20] F. H. Vaillancourt, D. A. Vosburg, C. T. Walsh, *ChemBioChem* **2006**, 7, 748–752.
- [21] S. P. Salowe, W. J. Krol, D. Iwata-Reuyl, C. A. Townsend, *Biochemistry* **1991**, 30, 2281–2292.
- [22] A. Goyal, P. Verma, M. Anandhakrishnan, R. S. Gokhale, R. Sankaranarayanan, *J. Mol. Biol.* **2012**, 416, 221–238.
- [23] R. D. Finn, C. G. Jones, *Nat. Prod. Rep.* **2003**, 20, 382–391.
- [24] G. D. Straganz, A. Slavica, H. Hofer, U. Mandl, W. Steiner, B. Nidetzky, *Biotransform.* **2005**, 23, 261–269.
- [25] G. D. Straganz, A. R. Diebold, S. Egger, B. Nidetzky, E. I. Solomon, *Biochemistry* **2010**, 49, 996–1004.
- [26] D. J. S. Hennessy, G. R. Reid, F. E. Smith, S. L. Thompson, *Can. J. Chem.* **1984**, 62, 721–724.
- [27] S. Leitgeb, G. D. Straganz, B. Nidetzky, *Biochem. J.* **2009**, 418, 403–411.
- [28] L. Whitmore, B. A. Wallace, *Nucleic Acids Res.* **2004**, 32, W668–W673.
- [29] J. J. La Clair, T. L. Foley, T. R. Schegg, C. M. Regan, M. D. Burkart, *Chem. Biol.* **2004**, 11, 195–201.
- [30] M. Zhao, J. Li, Z. Song, R. Desmond, D. M. Tschäen, E. J. J. Grabowski, P. J. Reider, *Tetrahedron Lett.* **1998**, 39, 5323–5326.

Received: May 29, 2013

Revised: October 28, 2013

Published online on February 4, 2014